Mesenchymal progenitors in osteopenias of diverse pathologies: differential features in the common shift from osteoblastogenesis to adipogenesis

Bingdong Sui[1, 2†], Chenghu Hu[1, 2†], Li Liao[1, 2], Yichen Chen[1, 2], Xinyi Zhang[1, 2], Xin Fu[1, 2], Chenxi Zheng[1, 2], Meng Li[1], Ling Wu[1, 2], Xinyi Zhao[3,4] & Yan Jin[1, 2*]

[1]State Key Laboratory of Military Stomatology, Center for Tissue Engineering, Fourth Military Medical University, Xi'an 710032, Shaanxi, China.

[2]Xi'an Institute of Tissue Engineering and Regenerative Medicine, Xi'an 710032, Shaanxi, China.

[3]Department of Dental Materials, School of Stomatology, Fourth Military Medical University, Xi'an 710032, Shaanxi, China.

[4]State Key Laboratory of Military Stomatology, Department of Dental Materials, Fourth Military Medical University, Xi'an 710032, Shaanxi, China.

[†]These authors contributed equally to this work.

[*]**Correspondence and requests for materials should be addressed to Prof. Yan Jin**

State Key Laboratory of Military Stomatology, Center for Tissue Engineering, Fourth Military Medical University, No. 145 West Changle Road, Xi'an, Shaanxi 710032, China. *E-mail:* yanjin@fmmu.edu.cn; *Tel:* +86-029-84776472; *Fax:* +86-029-83218039.

Journal: Scientific Reports.

Supplementary information: 11 figures and 1 table.

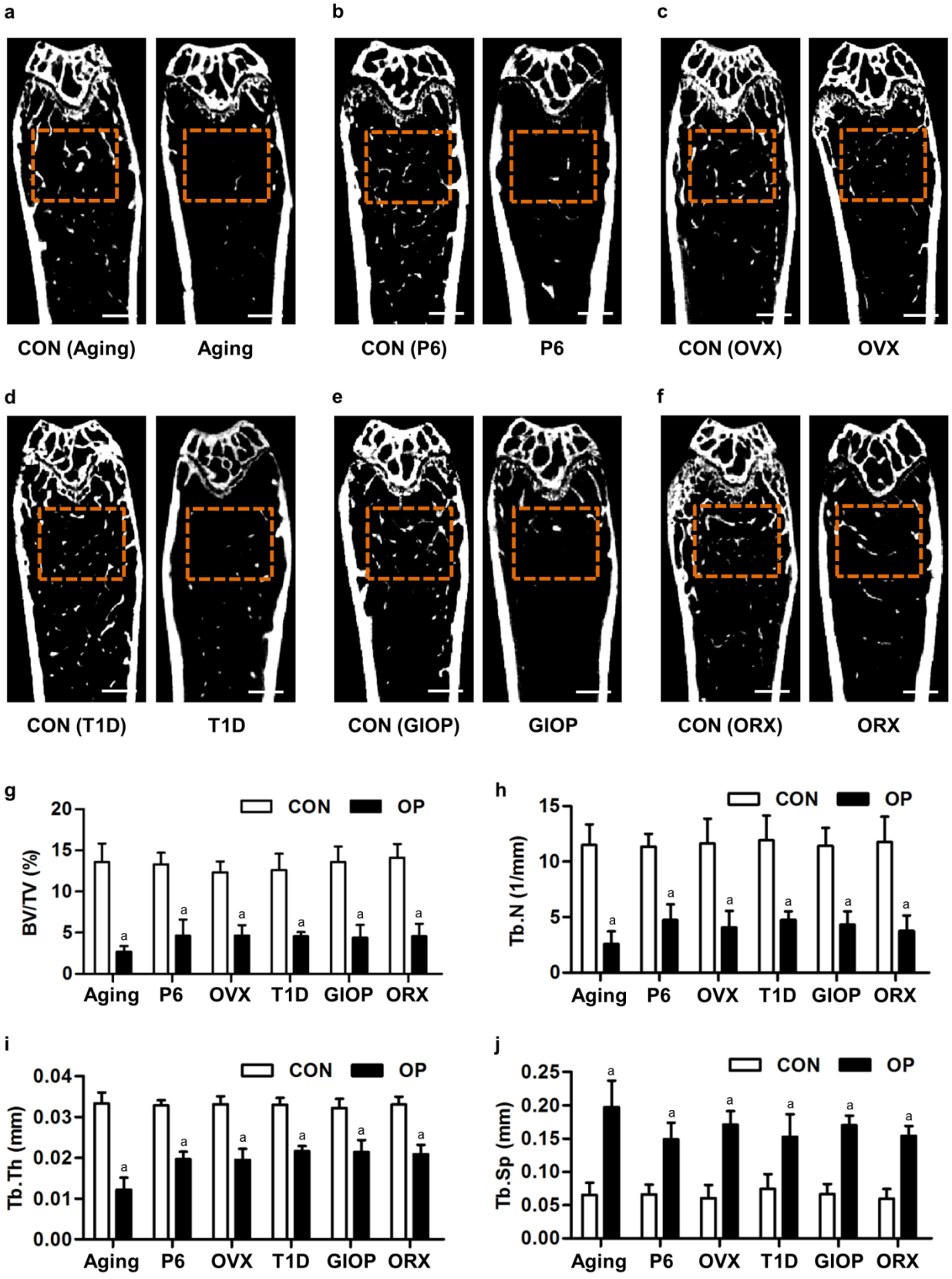

Supplementary Figure S1. The establishment of 6 different types of osteoporoses in mice. (**a-f**) Representative micro-CT images of the distal femora demonstrating successful establishment of 6 different

types of osteoporoses in mice. Mice were modeled 4 weeks for the control groups and osteoporoses induced by natural aging (**a**), accelerated senescence (SAMP6) (**b**), ovariectomy (OVX) (**c**), type 1 diabetes (T1D) (**d**), excessive glucocorticoids (GIOP) (**e**) and orchidectomy (ORX) (**f**). The orange boxes indicated the analyzed region of interest (ROI). Bars: 500 μm. (**g**) Analyzed by micro-CT, the parameter of bone volume over tissue volume (BV/TV) in the ROI demonstrating bone loss in the 6 types of osteoporoses. (**h-j**) Corresponding trabecular parameters of trabecular number (Tb.N) (**h**), trabecular thickness (Tb.Th) (**i**) and trabecular separation (Tb.Sp) (**j**) showing reduction of trabecular bone mass in 6 different types of osteoporoses. Data represents mean ± standard deviation (SD). n=6 per group. $^{a}P < 0.05$ with the control groups.

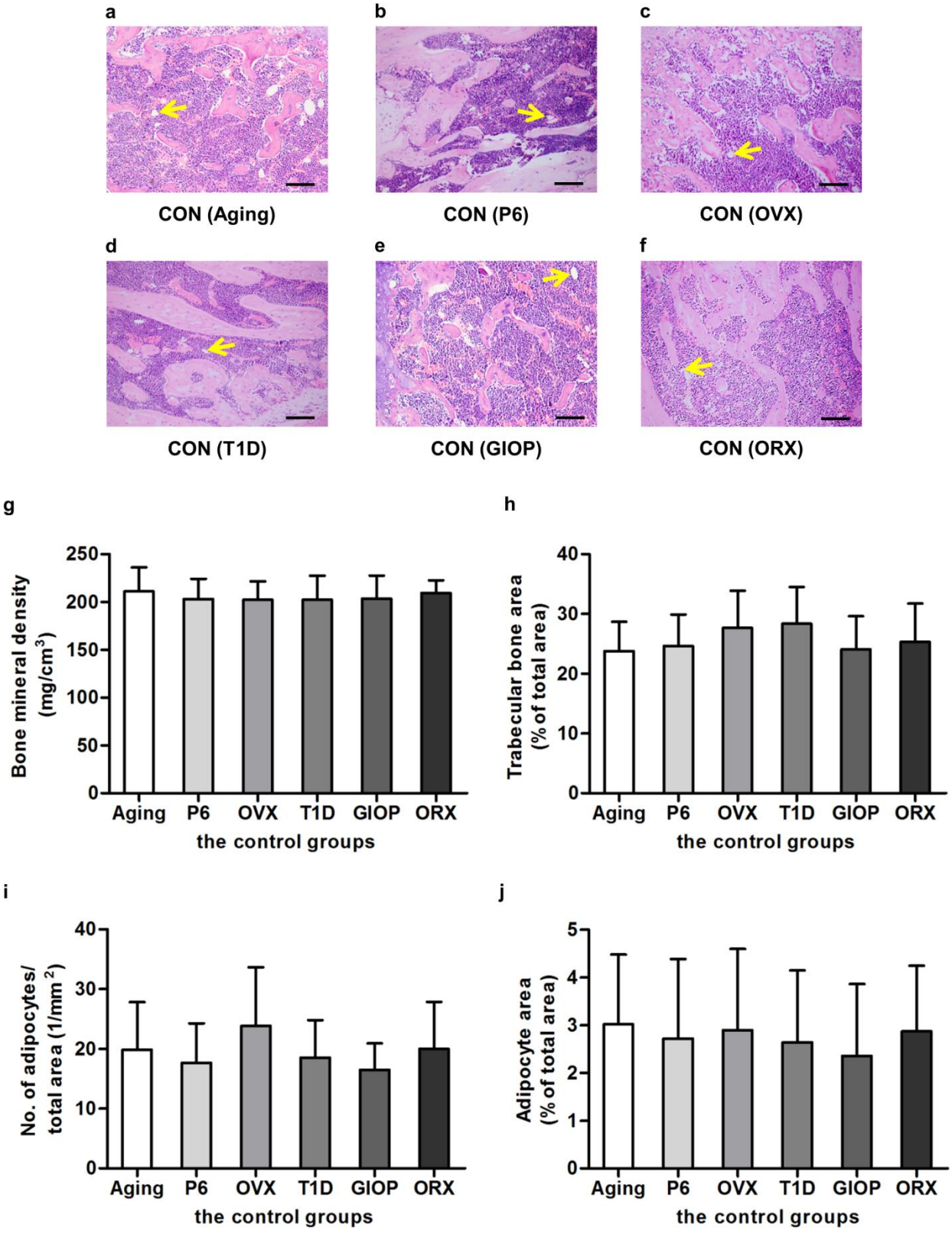

Supplementary Figure S2. Trabecular bone mass and marrow adiposity of the control groups. (**a-f**) Representative H&E images demonstrating trabecular bone and marrow adipose tissue in the distal femora of mice. Mice were modeled 4 weeks for the control groups of natural aging (**a**), accelerated senescence (SAMP6)

(**b**), ovariectomy (OVX) (**c**), type 1 diabetes (T1D) (**d**), excessive glucocorticoids (GIOP) (**e**) and orchidectomy (ORX) (**f**). The unstained area in the bone marrow represented empty spaces occupied by adipocytes with yellow arrows indicating. Bars: 100 μm. (**g**) Analyzed by micro-CT, the parameter of bone mineral density (BMD) in the distal metaphysis of femora demonstrating comparable bone mass in control groups of the 6 types of osteoporoses. (**h-j**) In bone histomorphometric analysis by H&E staining, the corresponding parameters of trabecular bone area over total area (**h**), number of adipocytes over total area (**i**) and adipocyte area over total area (**j**) showing paralleled bone mass and adipocytes in control groups of 6 different types of osteoporoses. Data represents mean ± standard deviation (SD). n=6 per group.

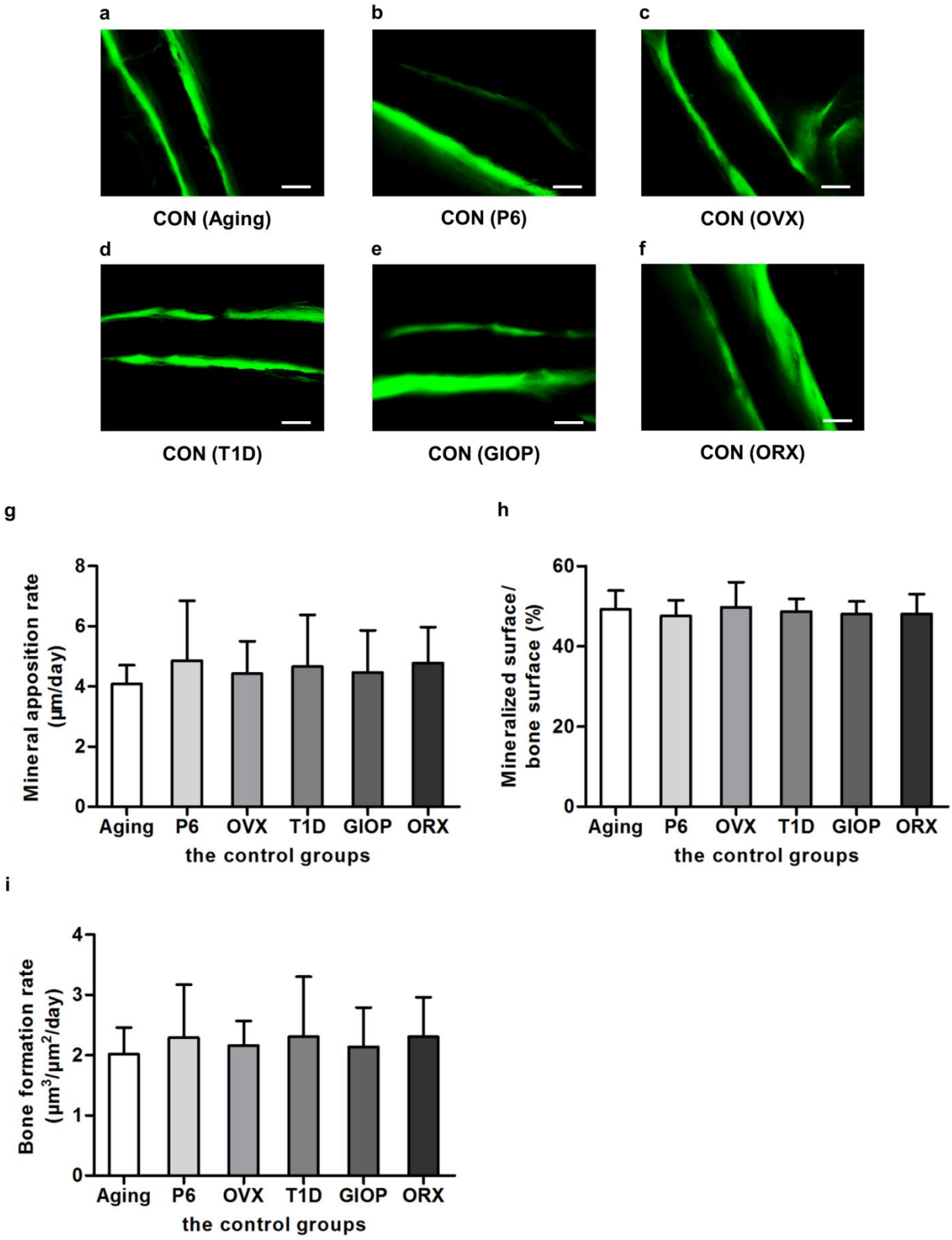

Supplementary Figure S3. Cortical bone formation parameters of the control groups. (**a-f**) Representative calcein labeling images demonstrating bone formation in the cortical endosteum of the distal femora of mice. Mice were modeled 4 weeks for the control groups of natural aging (**a**), accelerated

senescence (SAMP6) (**b**), ovariectomy (OVX) (**c**), type 1 diabetes (T1D) (**d**), excessive glucocorticoids (GIOP) (**e**) and orchidectomy (ORX) (**f**). Mice accepted double intraperitoneal injection of 20 mg/kg calcein at 16 days and 2 days prior sacrifice. Calcein was dissolved in PBS at 2 mg/ml supplemented with 1 mg/ml $NaHCO_3$. Bars: 100 µm. (**g-i**) The corresponding parameters of mineral apposition rate (**g**), mineralized surface over bone surface (**h**) and bone formation rate (**i**) showing comparable cortical bone formation in control groups of the 6 different types of osteoporoses. Data represents mean ± standard deviation (SD). n=6 per group.

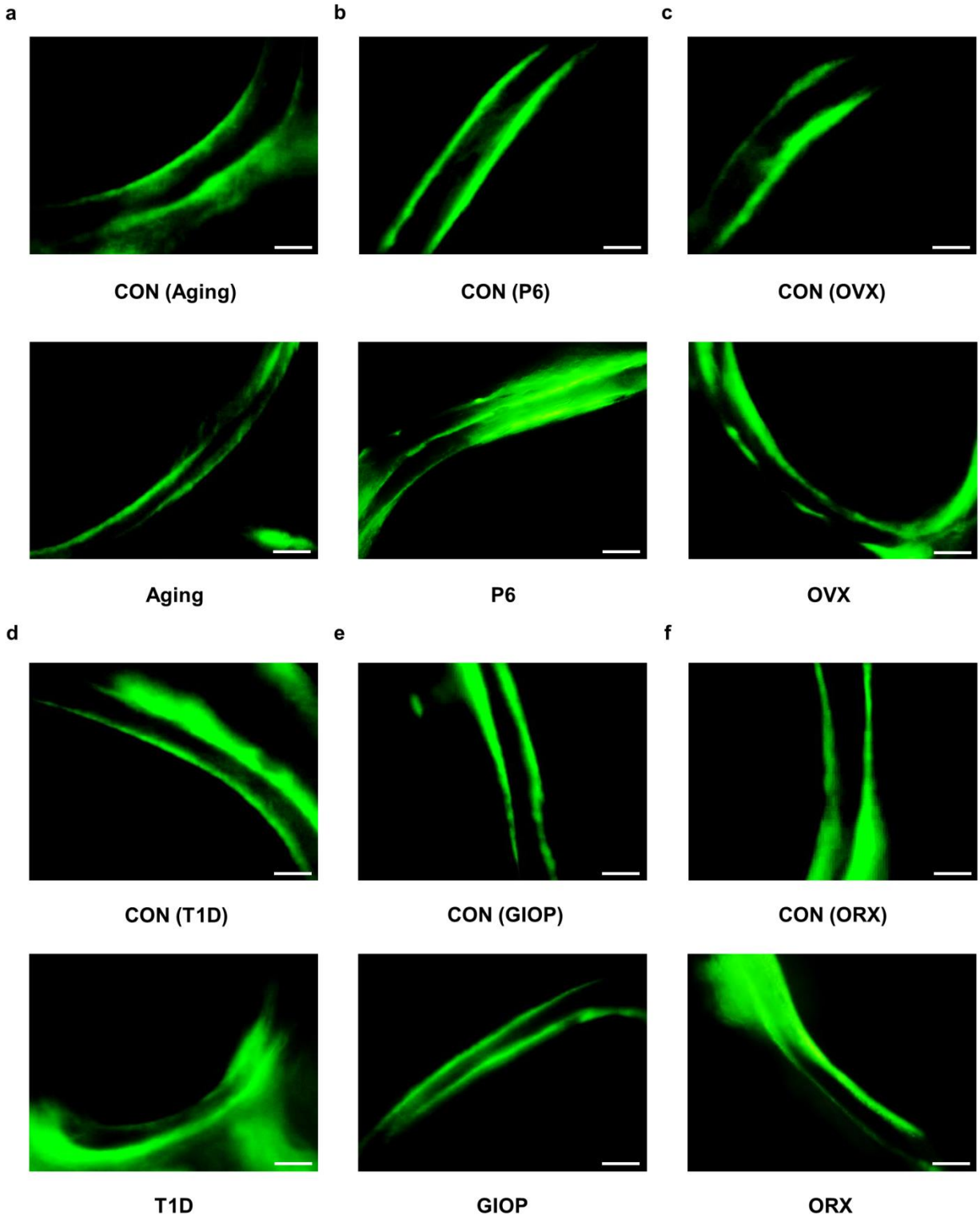

Supplementary Figure S4. Trabecular bone formation parameters. (**a-f**) Representative calcein labeling images demonstrating bone formation around the trabeculae of the distal femora of mice. Mice were modeled 4 weeks for the control groups and osteoporoses induced by natural aging (**a**), accelerated senescence (SAMP6)

(**b**), ovariectomy (OVX) (**c**), type 1 diabetes (T1D) (**d**), excessive glucocorticoids (GIOP) (**e**) and orchidectomy (ORX) (**f**). Mice accepted double intraperitoneal injection of 20 mg/kg calcein at 16 days and 2 days prior sacrifice. Calcein was dissolved in PBS at 2 mg/ml supplemented with 1 mg/ml $NaHCO_3$. Bars: 100 μm.

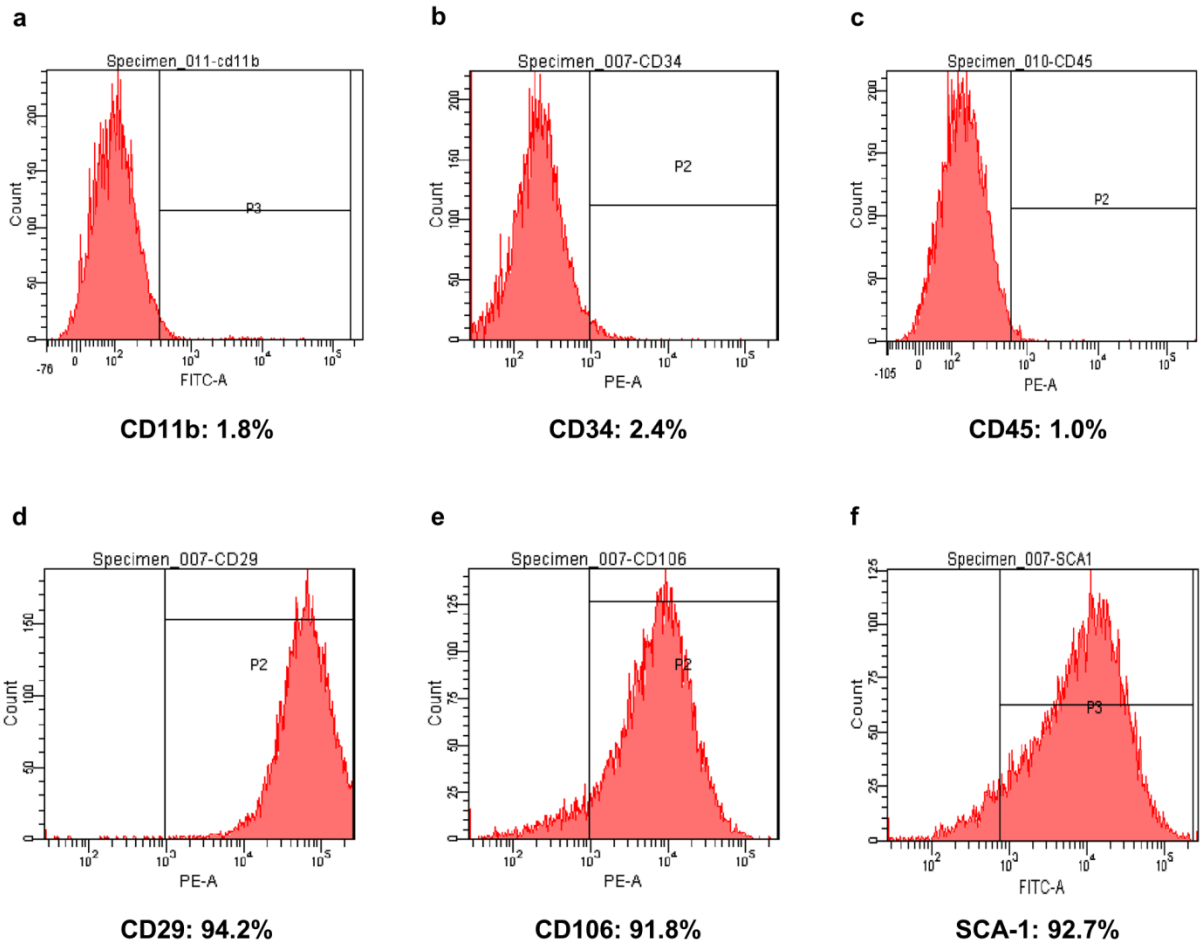

Supplementary Figure S5. Identification of surface markers of bone marrow stromal cells (BMSCs) used in the present study was in accordance with currently accepted standards. (**a-f**) Representative flow cytometric images demonstrating surface marker expression on BMSCs. BMSCs expressed surface makers considered to represent mesenchymal stem cells, including CD29, CD106 and stem cell antigen-1 (SCA-1), but were negative for hematopoietic markers CD11b, CD34 and CD45.

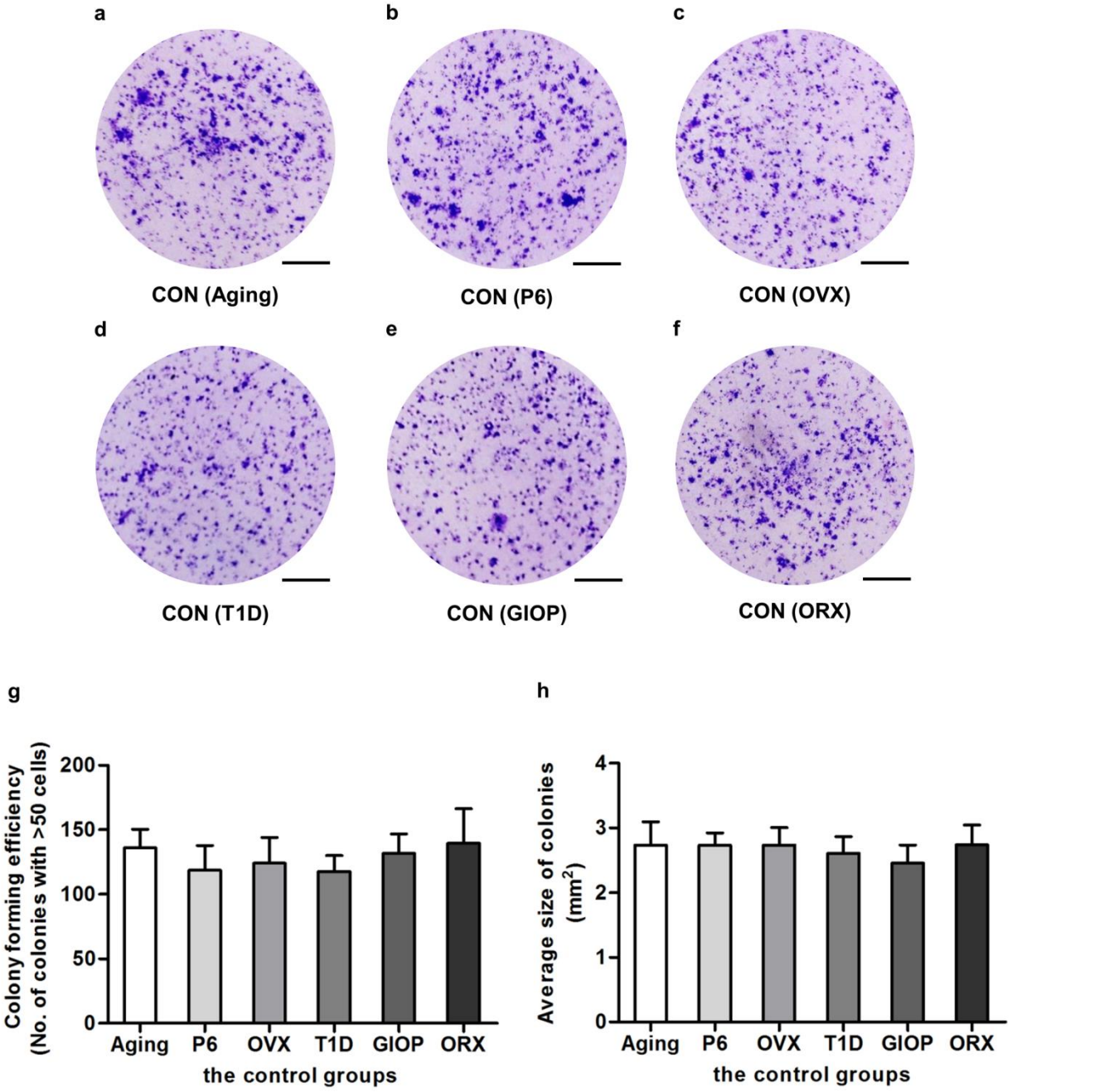

Supplementary Figure S6. Colony-forming efficiency of bone marrow stromal cells (BMSCs) derived from the control groups. (**a-f**) Representative images demonstrating colonies formed by primary murine BMSCs derived from the control groups of natural aging (**a**), accelerated senescence (SAMP6) (**b**), ovariectomy (OVX) (**c**), type 1 diabetes (T1D) (**d**), excessive glucocorticoids (GIOP) (**e**) and orchidectomy (ORX) (**f**). Mice were sacrificed after 4 weeks of modeling. Primary bone marrow cells were seeded at 1×10^5 cells/cm^2 after lysis of red blood cells. Bars: 1 cm. (**g, h**) The corresponding parameters of number of colonies

(**g**) and average size of colonies (**h**) showing paralleled colony-forming efficiency of BMSCs in control groups of the 6 different types of osteoporoses. Colonies with over 50 cells were taken into consideration. Data represents mean ± standard deviation (SD). n=6 per group.

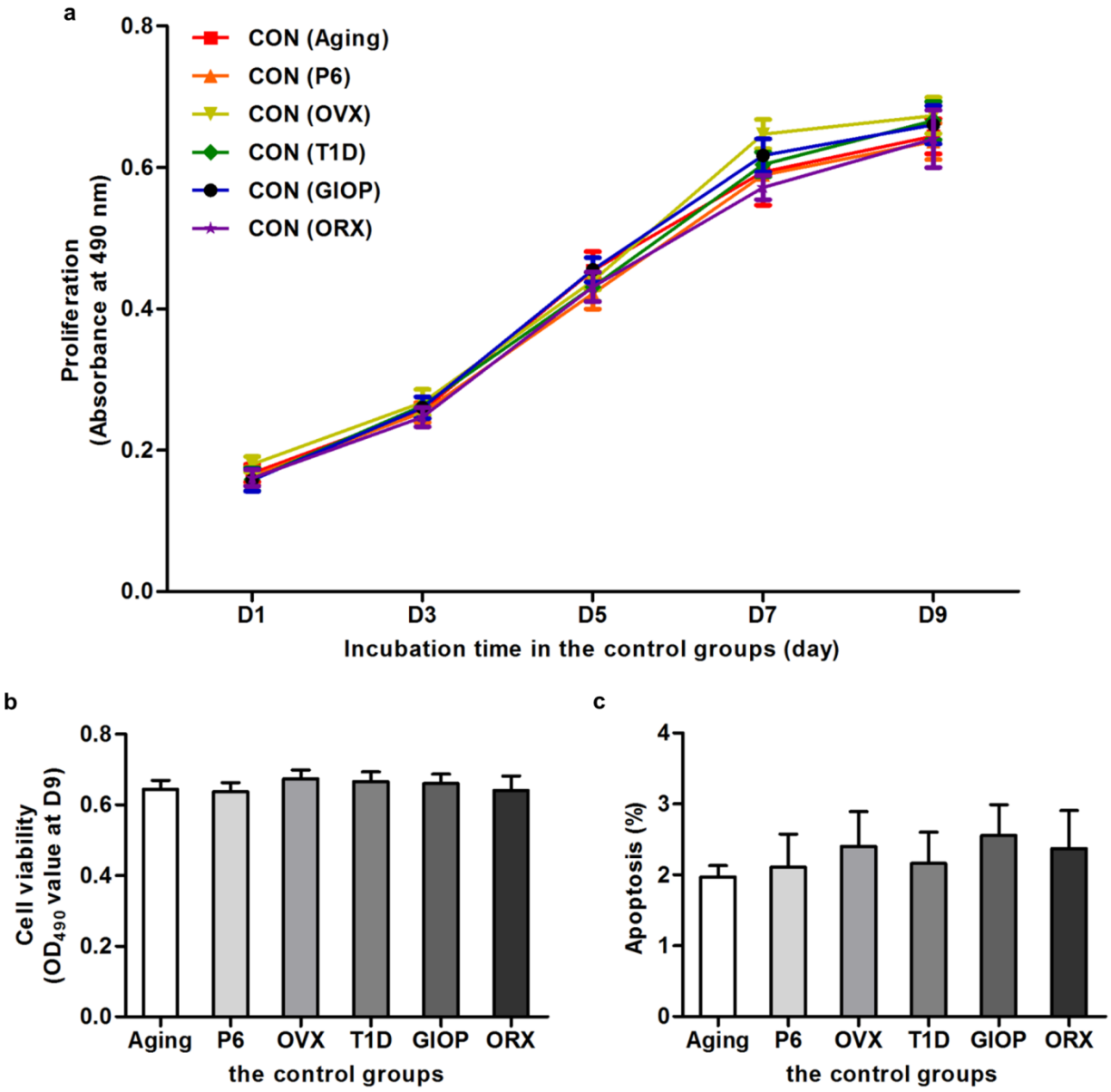

Supplementary Figure S7. Proliferation rate and apoptosis of bone marrow stromal cells (BMSCs) derived from the control groups. (**a**) Representative MTT curves demonstrating proliferation of murine BMSCs derived from the control groups of natural aging, accelerated senescence (SAMP6), ovariectomy (OVX), type 1 diabetes (T1D), excessive glucocorticoids (GIOP) and orchidectomy (ORX). Mice were sacrificed after 4 weeks of modeling. 1st-passaged BMSCs were seeded at 2 × 10^3 cells/well in 96-well plates and the cell viability was evaluated at the same time points in Day-1, 3, 5, 7, and 9. (**b**) The values of optical density at 490 nm in the MTT test at Day-9 showing similar proliferation rate of BMSCs in the control groups. (**c**)

Flow cytometry analysis showed similar apoptosis of BMSCs in the control groups. 1st passaged BMSCs were harvested 3 days after seeding and evaluated by FITC-conjugated Annexin V and propidium iodide (PI) double staining, and the percentages of early apoptotic ($FITC^+PI^-$) plus late apoptotic/necrotic ($FITC^+PI^+$) cells were expressed as apoptotic BMSC percentages. Representative flow cytometry plots for the controls were shown in Supplementary Figure S7. Data represents mean ± standard deviation (SD). n=6 per group.

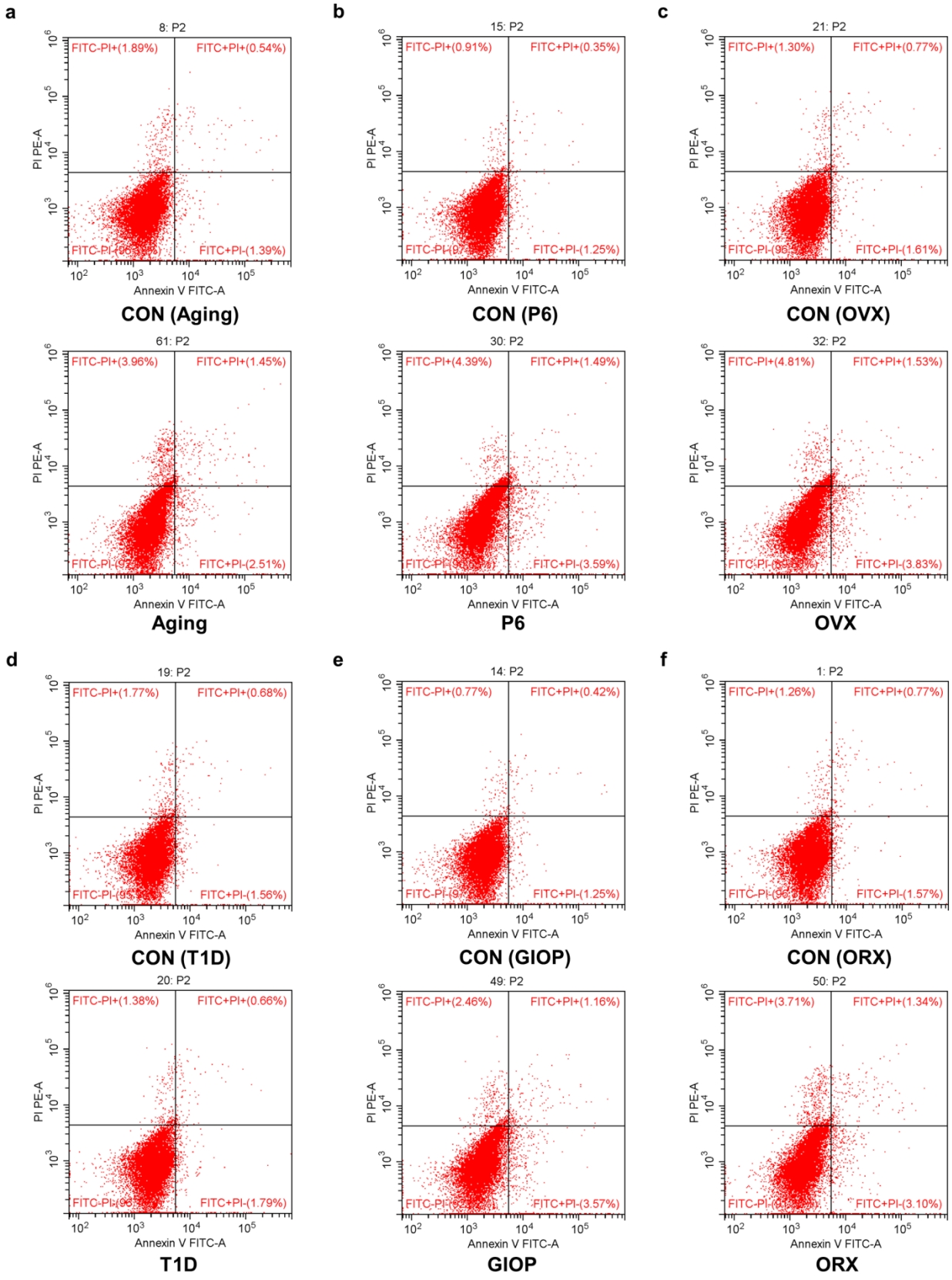

Supplementary Figure S8. Apoptosis of bone marrow stromal cells (BMSCs). (**a-f**) Representative flow cytometric images of BMSCs demonstrating apoptosis evaluated by FITC-conjugated Annexin V and

propidium iodide (PI) double staining. Mice were modeled 4 weeks for the control groups and osteoporoses induced by natural aging (**a**), accelerated senescence (SAMP6) (**b**), ovariectomy (OVX) (**c**), type 1 diabetes (T1D) (**d**), excessive glucocorticoids (GIOP) (**e**) and orchidectomy (ORX) (**f**). The percentages of early apoptotic ($FITC^{+}PI^{-}$) plus late apoptotic/necrotic ($FITC^{+}PI^{+}$) cells were expressed as apoptotic BMSC percentages.

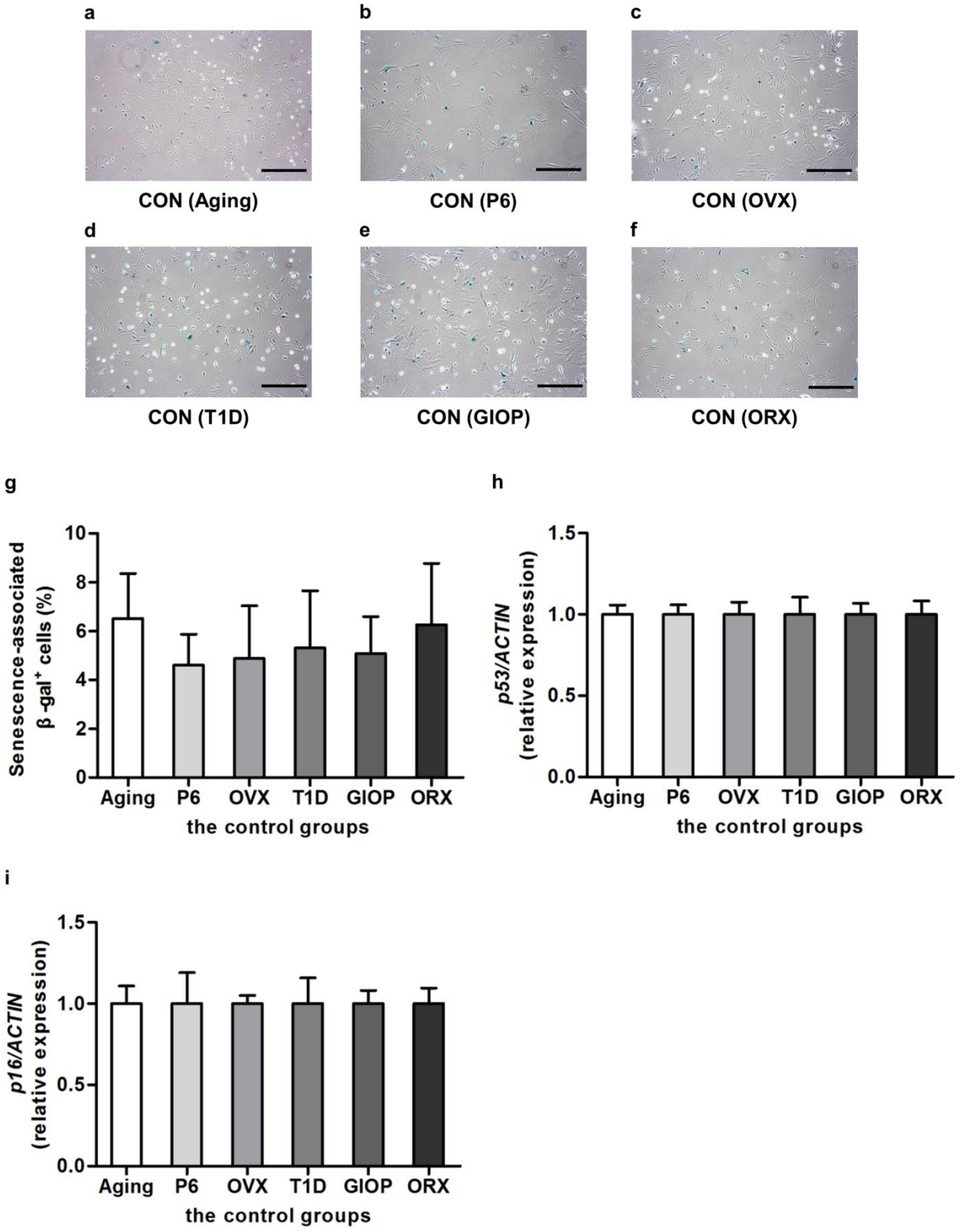

Supplementary Figure S9. Cellular senescence of bone marrow stromal cells (BMSCs) derived from the control groups. (**a-f**) Representative β-galactosidase (β-gal) staining images demonstrating cellular senescence of murine BMSCs derived from the control groups of natural aging (**a**), accelerated senescence

(SAMP6) (**b**), ovariectomy (OVX) (**c**), type 1 diabetes (T1D) (**d**), excessive glucocorticoids (GIOP) (**e**) and orchidectomy (ORX) (**f**). Mice were sacrificed after 4 weeks of modeling. 1^{st}-passaged BMSCs were seeded at 1×10^5 cells/well in 12-well plates and were stained for β-gal. The senescent cells were positively stained (green). Bars: 200 μm. (**g**) The corresponding percentage of senescence-associated β-gal positive cells over total cells showing paralleled senescence of BMSCs in control groups of the 6 different types of osteoporoses. (**h, i**) Quantitative real-time polymerase chain reaction (qRT-PCR) analysis of the mRNA expression level of *p53* and *p16*. The corresponding values were not significantly different among the control groups. The expressions of *p53* and *p16* were normalized to that of *ACTIN*. Data represents mean ± standard deviation (SD). n=6 per group.

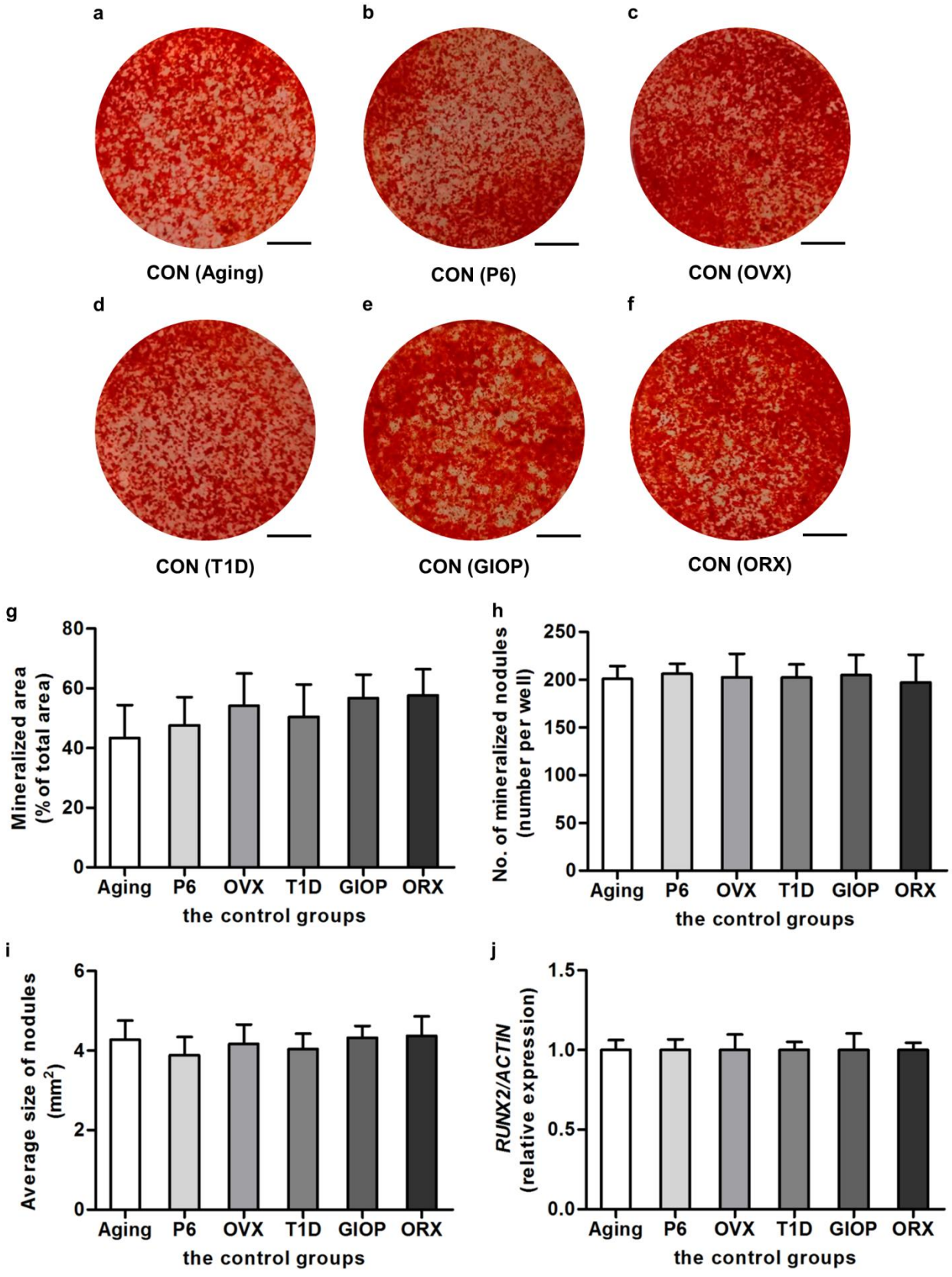

Supplementary Figure S10. Osteogenic differentiation of bone marrow stromal cells (BMSCs) derived from the control groups. (**a-f**) Representative alizarin red staining images demonstrating mineralization by

murine BMSCs derived from the control groups of natural aging (**a**), accelerated senescence (SAMP6) (**b**), ovariectomy (OVX) (**c**), type 1 diabetes (T1D) (**d**), excessive glucocorticoids (GIOP) (**e**) and orchidectomy (ORX) (**f**). Mice were sacrificed after 4 weeks of modeling. 1^{st}-passaged BMSCs were seeded at 2×10^5 cells/well in 12-well plates and underwent osteogenic induction for 14 days. Bars: 5 mm. (**g-i**) The corresponding parameters of mineralized area over total area (**g**), number of mineralized nodules per well (**h**) and average size of nodules (**i**) showing comparable mineralization of BMSCs in control groups of the 6 different types of osteoporoses. (**j**) After 14-day osteogenic induction, quantitative real-time polymerase chain reaction (qRT-PCR) analysis of the mRNA expression level of osteogenic marker gene *Runt-related transcription factor 2 (RUNX2)*. The corresponding values were not significantly different among the control groups. The expression of *RUNX2* was normalized to that of *ACTIN*. Data represents mean ± standard deviation (SD). n=6 per group.

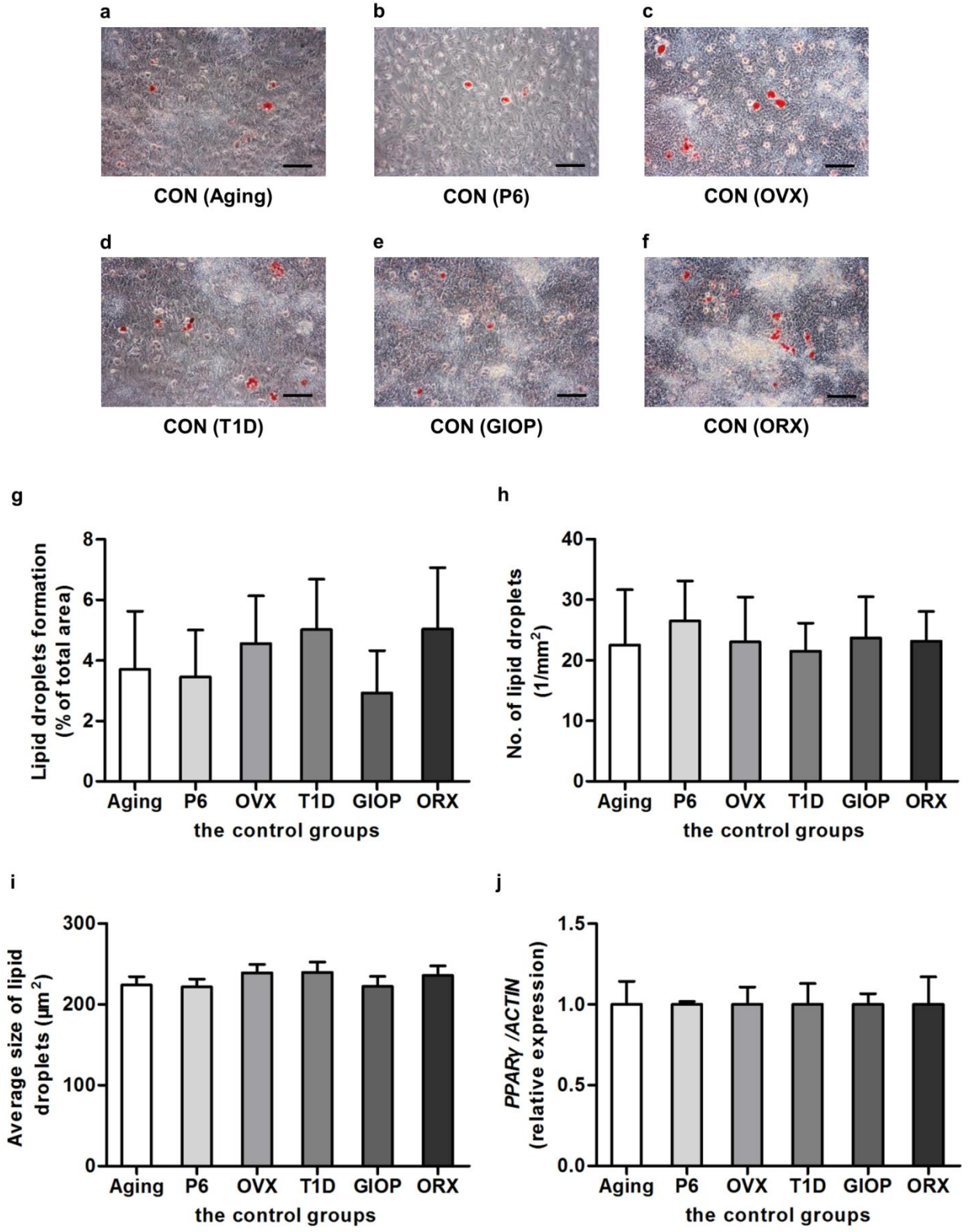

Supplementary Figure S11. Adipogenic differentiation of bone marrow stromal cells (BMSCs) derived from the control groups. (**a-f**) Representative oil red O staining images demonstrating formation of lipid droplets by murine BMSCs derived from the control groups of natural aging (**a**), accelerated senescence

(SAMP6) (**b**), ovariectomy (OVX) (**c**), type 1 diabetes (T1D) (**d**), excessive glucocorticoids (GIOP) (**e**) and orchidectomy (ORX) (**f**). Mice were sacrificed after 4 weeks of modeling. 1^{st}-passaged BMSCs were seeded at 2×10^5 cells/well in 12-well plates and underwent adipogenic induction for 14 days. Bars: 100 μm. (**g-i**) The corresponding parameters of lipid droplets formation over total area (**g**), number of lipid droplets per square millimeter (**h**) and average size of lipid droplets (**i**) showing paralleled adipogenic differentiation of BMSCs in control groups of the 6 different types of osteoporoses. (**j**) After 14-day adipogenic induction, quantitative real-time polymerase chain reaction (qRT-PCR) analysis of the mRNA expression level of adipogenic marker gene *Peroxisome proliferator activated receptor gamma (PPARγ)*. The corresponding values were not significantly different among the control groups. The expression of *PPARγ* was normalized to that of *ACTIN*. Data represents mean ± standard deviation (SD). n=6 per group.

Supplementary Table S1. Primer sequences in the present study.

Gene	Primer sequences
ACTIN	Forward: 5’-CATCCGTAAAGACCTCTATGCCAAC-3’
	Reverse: 5’-ATGGAGCCACCGATCCACA-3’
p53	Forward: 5’-ATGGTCAAGAAAGTGGGGCCT-3’
	Reverse: 5’-TGAGTGGATCCTGGGGATTGT-3’
p16	Forward: 5’-CTCACCTCGCTTGTCACAGT-3’
	Reverse: 5’-TCGCACGAACTTCACCAAGA-3’
RUNX2	Forward: 5’-AAATGCCTCCGCTGTTATGAA-3’
	Reverse: 5’-AAGGTGAAACTCTTGCCTCGTC-3’
PPARγ	Forward: 5’-TGTGAGACCAACAGCCTGAC-3’
	Reverse: 5’-AAGTTGGTGGGCCAGAATGG-3’